

ESTIMATION OF COMPRESSIVE STRENGTH OF LIGHT WEIGHT FOAMED CONCRETE USING ARTIFICIAL INTELLIGENCE

Saurav¹, Dr.S.Thenmozhi², Dr. Hemadri Prasad Raju³, Dinesh W Gawatre⁴, Kuldeep Pathak⁵

¹Assistant professor, Department of civil engineering, Bhagalpur college of engineering Bhagalpur Sabour Bihar 813210, sauravkumar550@gmail.com

²Associate Professor, Department of Civil Engineering, St. Joseph's College of Engineering, OMR, Chennai 600 119.

³Associate Professor, Department of Civil Engineering, Mohan Babu University (Erstwhile Sree Vidyanikethan Engineering College), Sree Sainath Nagar, Tirupati, Andhra Pradesh. PIN:517102.

⁴Assistant Professor, Department of Civil Engineering, Sinhgad Academy of Engineering, Pune-411048, (SPPU-Pune University) Maharashtra-India

⁵Assistant Professor, Department of Civil Engineering, Vikrant University, Gwalior, 474006, Madhya Pradesh

ABSTRACT: Foamed concrete is exceptional not only for its distinctive features but also for the complex compositional mixture design that calls for several experimental attempts to achieve the required attribute, such as compressive strength. Despite the difficulties in design, artificial intelligence (AI) methods have proven to be effective in accurately calculating required concrete qualities based on optimised mixing proportions. In order to forecast the compressive strength of foamed concrete, this study suggests AI-based models. Artificial neural network (ANN), gene expression programming (GEP), and gradient boosting tree (GBT) models were three cutting-edge AI techniques used. The models were created utilising data from 232 experiments, considering readily available factors such as concrete density, water-to-cement ratio, and sand-to-cement ratio as inputs to calculate the compressive strength of foamed materials. 80% of the experimental data was utilised to train the models, while the remaining 20% was used to verify the models. On a trial-and-error basis, the optimised models were chosen using their respective best hyper-parameters; for ANN, variable numbers of hidden layers, neurons, and training algorithms were used; for GEP and GBT, variable numbers of chromosomes, head sizes, and genes were used; and variable numbers of trees, maximal depths, and learning rates were employed. Using parametric and sensitivity analysis on a simulated dataset, the trained models were verified. The coefficient of correlation (R), mean absolute error (MAE), and root mean squared error (RMSE) were used to assess the suggested models' predictive power.

Keywords: Foamed concrete Lightweight concrete Artificial neural network Gene expression programming Gradient boosting tree Optimization

1 INTRODUCTION

Due of concrete's superior composite behaviour with steel, reinforced concrete buildings frequently employ it as a construction material. To alter concrete's mechanical and durability characteristics, a variety of substitutions are used in lieu of (partially or entirely) the original materials [1, 2]. Foamed concrete (FC) is a light cellular concrete with randomly filled air holes in the binding mortar, which accounts for its decreased self-weight [4]. Its density ranges between 300 and 1850 kg/m³ [3]. Additionally to FCs, these materials are also referred to as low-density FC, cellular LW concrete, and LW cellular concrete [5-8]. Be aware that while the FC material is by no means a novel invention, it has gained favour recently as a more affordable and environmentally friendly concrete substitute [9]. They have been employed to create LW buildings that are earthquake and fire resistant [10,11]. Cement, fine and coarse aggregates, water, and foaming additives are the ingredients of FC, which gives concrete its

"LW behaviour." Many studies have included binder supplements in addition to the aforementioned conventional components, such as industrial waste glass and rubber [12,13], eggshell waste [14–16], and sawdust [17]. These add-on components serve as the FC's "diets," portraying it as a remedy for various social and economic problems in addition to improving its physical attributes [18]. The types of foaming agents, cement mineralogy, and aggregate granulometry, as well as pore nature and regularity, water quality, the quantity of the component elements in the mixture, and the chosen curing techniques, all have an impact on these qualities [19]. According to reports for typical concrete [20], a higher cement percentage is often equivalent to a higher compressive strength. In the case of FCs, a similar tendency may be shown; however, when the cement concentration surpasses 500 kg/m³, a decline in strength is seen [21]. Additionally, a greener FC was created by partially substituting extra cementitious materials for cement [22]. The presence of air bubbles from a solution of water, foaming agents, and pressurised air is what gives ordinary FC its LW character [3]. Detergents, glue resins, hydrolyzed proteins, protein-based resin soap, saponins, and synthetic agents are all readily accessible foaming agents; however, synthetic and protein-based foaming agents are more often used [23,24]. There is no precise mixture proportioning process that may be used to attain a certain attribute of foamed concrete effectively. However, it generally takes multiple trial-and-error sessions to find the ideal blend utilising parameters like binder content, percentage foam content, and net water content [23,25]. When the right combinations are used, FCs have excellent properties such a high strength-to-weight ratio and low density that help reduce dead loads, foundation size, and construction costs for labour, material transport, and operation [26–28]. Additionally, the FCs have improved sound absorption, high thermal conductivity, balanced energy conservation, and fire resistance due to their textured surface and cellular microstructure [4,29]. Due to their numerous high-level and distinctive qualities, including density reduction, FCs are considered green LW structural materials in building and road construction projects. FC is preferable to other LW structural materials like dry walls and wood due to the inherent environmental challenges associated with their production process as well as their high costs. Some of the key characteristics that have enhanced the use of FCs in several civil infrastructure and structural applications are low density, thermal conductivity, and cost efficiency [30,31]. Examples include cavity filling and insulation, LW precast concrete blocks and panels, insulation against heat, sound, and fire, soil stabilisation, shock-absorbing airport barriers, and regular traffic on the roads [30–34]. The FCs are an excellent candidate for void filling due to their remarkable rheology, notably in collapsing sewers, ducts, and voids underneath roads [33]. Additionally, FCs are becoming more and more well-liked on a worldwide scale, with particular appeal in regions that are facing a housing crisis or severe weather. There are a lot of FCs. consumed per year in both wealthy and underdeveloped countries, including the UK (250,000–300,000 m³), western Canada (around 50,000 m³), and Korea (250,000 m³) in order to address concerns about load reduction, thermal insulation, structural stability, temperature variations, floor heating systems, and the costs of repair and maintenance [33, 35–38]. The structural loads (dead, living, wind, etc.) must be resisted during building design, making them crucial elements to take into account. A significant number of large, tall structures have been built recently all over the world [39], and the reduction of structural loads is a recurrent problem among designers and practitioners. Balancing the strength needs of the LW concrete for structural purposes from the perspective of structural materials

The compressive strength of FC is one of its most crucial properties since it indicates how well it can withstand stresses before failing. This emphasises the significance of the compressive strength characteristic even more. Through the performance traits of its components, FC's density directly affects its compressive strength. The FC's compressive strength and density are directly correlated with one another [41]. Flexural and tensile strengths are related to each other in this way. As the FC's density declines, other characteristics, such as its durability performance [42–44], pore structural properties [45–46], fracture properties [47], and other mechanical strength properties [48–51], also tend to do the same. The water-to-binder ratio, sand-to-binder ratio, curing time, void distribution, and kind of foaming agent

are the main factors impacting the FCs' strength attributes [52]. The compressive strength qualities were impacted by the addition of additives and admixtures, and further aspects included air void size and form (void structure), dosage of admixtures, and the percentage of additive substitution for cement [53,54].

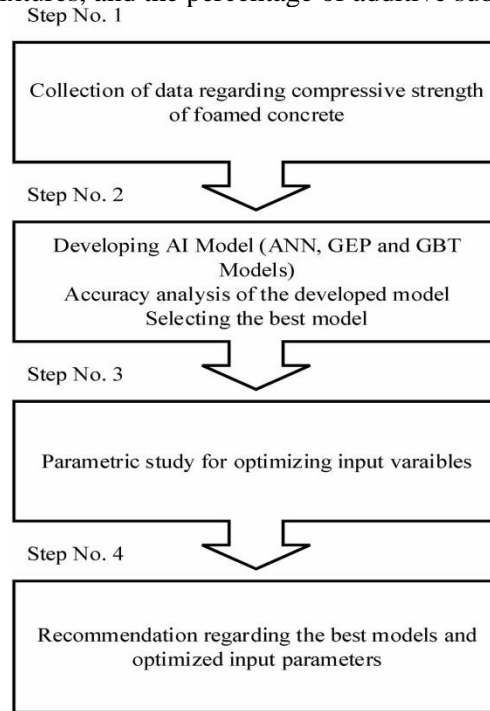


Fig. 1. Adopted methodology for the current research to evaluate the compressive strength of foamed concrete.

The fundamental models developed by Balshin, Feret, and Power were the key sources of inspiration for earlier empirical models that forecast the compressive strength of FCs [20]. The compressive strength of FC and the volume of voids in concrete are related by Balshin's model. Power's approach links strength to the gel-space ratio, whereas Feret's model links the compressive strength of the FC to the absolute volume of the constituent [58]. These empirical models' detailed derivations are available in the published literature [59]. The majority of empirical models used to estimate the compressive strength of FCs are calibrated using experimental data and only use a small number of input parameters when creating their equations, which means that the majority of their predictions are extrapolative [60]. Designing an FC mixture to achieve a target or required compressive strength is particularly complex; for example, reports have shown distinct differences in the compressive strength between protein-based foam agents and synthetic foam agents, with the former generally having a greater influence [62,63]. In contrast to others, the creation of air bubbles by the foaming agents has a significant influence on several mechanical qualities. Additionally, due to the foaming agent's increased stability during blending, air bubbles have a bigger impact on FC's compressive strength than its modulus of elasticity [64]. It is important to note that it would be challenging to use empirical and numerical approaches to describe this complexity, and the resulting models would not be appropriate to predict the intended objectives with a respectable level of accuracy. Currently, the most crucial necessity in the LW concrete study is early judgements on the FC mixture design to precisely reach a specific compressive strength. This necessitates the use of increasingly potent and sophisticated prediction tools, such machine learning (ML) algorithms. The complexity of the FC mixture proportioning, which typically prevents the empirical equations from accurately predicting the necessary concrete qualities, may be handled by the ML algorithms due to built-in capabilities [65]. Additionally, since ML algorithms are not constrained by human physics expertise,

they offer more accurate predictions than conventional approaches like mathematical modelling or trial-and-error. For analytics and forecasts, these approaches have become a crucial component of civil and structural engineering [66–70]. Current research is largely focused on utilising ML for predictive modelling to design and forecast the compressive strength of various types of concrete prior to casting, which would significantly minimise waste from laboratory experiments before obtaining the best combinations [66,71–73]. The behaviour of concrete structures under various situations has also been modelled using these algorithms [74].

Table 1 Description of input and target parameters for model development.

	Variable	Description	Unit	Max	Min	Standard deviation	Range
Input	Density	Density of concrete	Kg/m ³	2065.60	430.00	417.71	1635.60
	w/c	Water to cement ratio	–	0.83	0.26	0.13	0.57
	s/c	Sand to cement ratio	–	4.29	0.00	0.72	4.29
Target	CS	Compressive strength	MPa	51.18	1.50	13.93	49.68

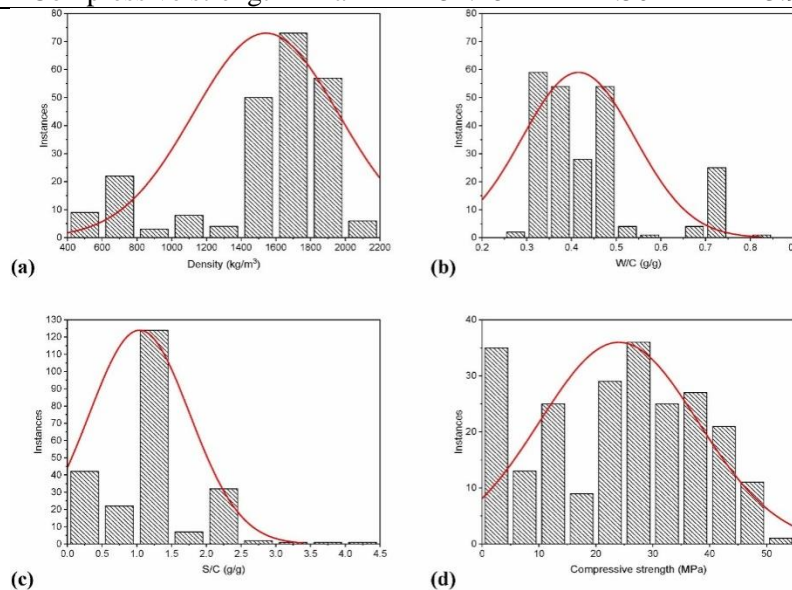


Fig. 2. Distribution histograms of the input and output variables used in the study.

Table 2 Linear Pearson’s correlation between inputs and the target variable.

Attribute	Compressive strength	Density	S/C	W/C
Compressive strength	1.000	0.879	0.023	–
Density	0.879	1.000	0.328	–
S/C	0.023	0.328	1.000	–
W/C	–0.587	–0.517	–	1.000
			0.068	

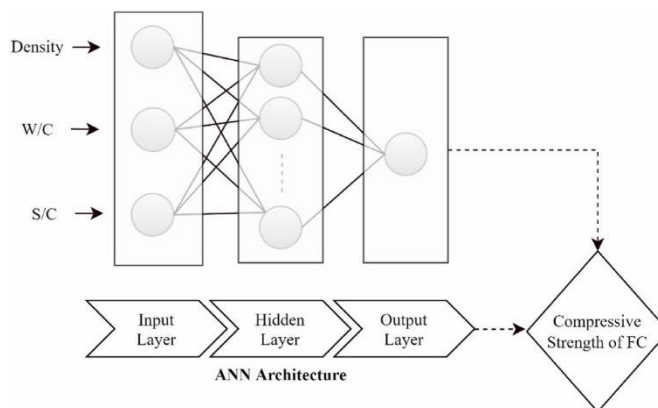


Fig. 3. The architecture of proposed ANN model to evaluate the compression strength of Foamed concrete.

FCs. Without assessing fresh data based on the established models, the majority of research evaluated the performance of the prediction models for the improvement of input parameters. In order to properly forecast the attributes of the FCs, it is also necessary to elaborate on and demonstrate the capabilities of other methodologies, particularly novel evolutionary paradigms like gene expression programming (GEP) and ensemble models like gradient boost tree (GBT). Three potent ML algorithms—ANN, GEP, and GBT—with significant nonlinear capabilities are used in this work to forecast the compressive strength. To achieve the desired density, the water-to-cement and sand-to-cement ratios have been optimised using parametric analysis. A succinct description of the issue is followed by The experimental database utilised in the creation of the models, the selection of the variables, and a succinct description of the employed predictive modelling and AI models. Section 3 contains the findings and discussion, which show how well the constructed models work as well as parametric and sensitivity evaluations of each contributing variable. The main findings of this investigation are then discussed. In order to attain the necessary compressive strength as required by applications, the proposed models would be used to choose the best mixture design option for foamed concrete.

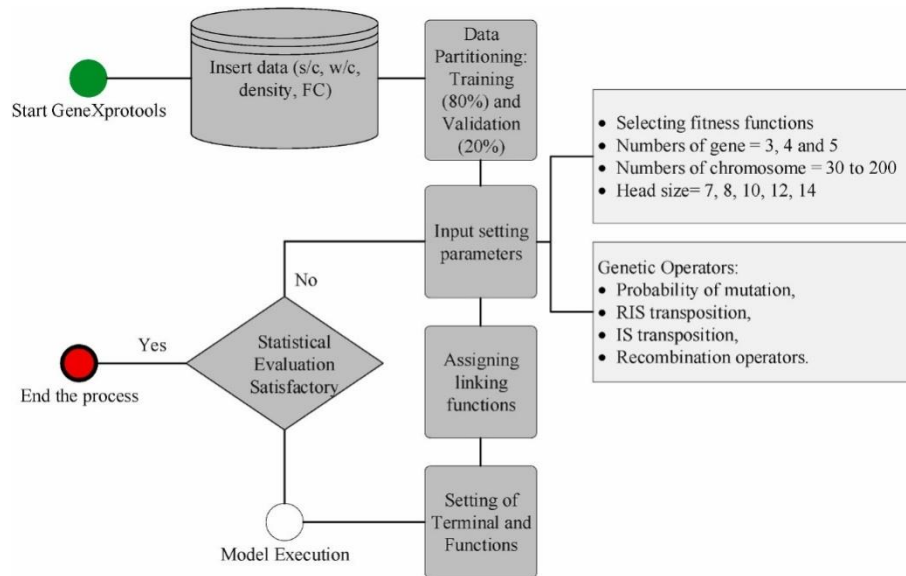


Fig. 4. GEP Prediction modelling of compression strength of Foamed concrete using GeneXProtocols

Table 4 Statistical evaluation of the developed multiple models based on variable setting parameters.

Model No.	Variable setting parameters		Training dataset				Validation dataset			
	Fitness function	Number of chromosomes, head size, genes	Correlation (R)	RMSE	MAE	RSE	Correlation (R)	RMSE	MAE	RSE
GEP1	RMSE	30, 7, 3	0.963	3.818	3.040	0.072	0.947	4.054	3.417	0.103
GEP2	RMSE	30,8,3	0.954	4.093	3.353	0.090	0.961	4.204	3.516	0.080
GEP3	RMSE	50,10,4	0.957	3.997	3.253	0.085	0.961	4.242	3.563	0.082
GEP4	RMSE	200,12,5	0.971	3.238	2.751	0.056	0.951	3.401	2.695	0.052
GEP5	RMSE	200,14,5	0.940	3.706	3.706	0.116	0.936	5.318	4.252	0.128

2 RESEARCH METHODOLOGY

The approach used for the current study is shown in Fig. 1. For the purpose of creating AI models, data was gathered on the compressive strength of foamed concrete. Due to their better non-linear capabilities reported in the earlier research [78–80], ANN, GEP, and GBT models were used. Iqbal et al. [81] previously used the approach that was used in this investigation. The produced models were evaluated in order to choose a more reliable model, which was then put through parametric analysis in order to optimize the input parameters. Here is a quick introduction to experimental databases and AI models. This part also provides an explanation of the intricate AI modelling.

Experimental database

It is essential to create a thorough and well-designed database, a precise and detailed description of the database, statistically analysed input variables, and insights into the datasets in order to create a powerful machine-learning model. In order to train the three algorithms used for this work, a database of cleaned data made up of 232 experimental test results for foamed concrete was constructed from international publications by various researchers [82-87]. The dataset includes several foamed concrete mixes with compressive strength (CS) as the output parameter and input values for density, water-to-cement (w/c) ratio, and sand-to-cement (s/c) ratio. Table 1 contains a list of the input and target factors (experimental design variables) utilised in the investigation. The distribution of the input and target parameters

throughout model development is depicted in Fig. 2. These graphs are especially useful since they may help identify parameter values for which there aren't enough data and more are needed [88]. The majority of the data points exhibit densities between 1400 and 2000 kg/m³ (Fig. 2a), w/c ratios between 0.3 and 0.5 (Fig. 2b), and s/c ratios between 0.5 and 2.0 (Fig. 2c), as can be observed. It is advised that the produced models be applied inside of these input restrictions. The correlation coefficients between all variables examined were computed and are shown in Table 2 as a result of the input parameters' interdependence. A quick analysis of the relationships between the input variables revealed that the density had a high positive correlation with the compressive strength whereas the w/c ratio had a large negative association. The compressive strength of the foam concrete showed a somewhat negative connection with the sand-to-cement ratio (s/c). Because there are connections between the input and target characteristics, it is possible for the suggested algorithms to learn these relationships quickly and effectively, which results in accurate compressive strength prediction.

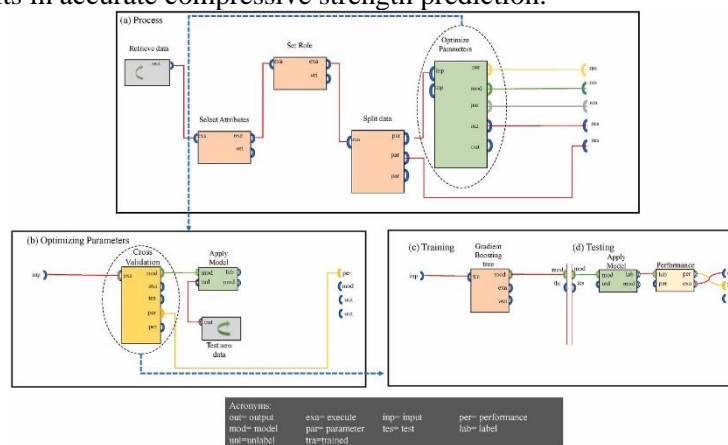


Fig. 5. Flow diagram depicting GBT modelling (Adapted from Iqbal et al. [81]).

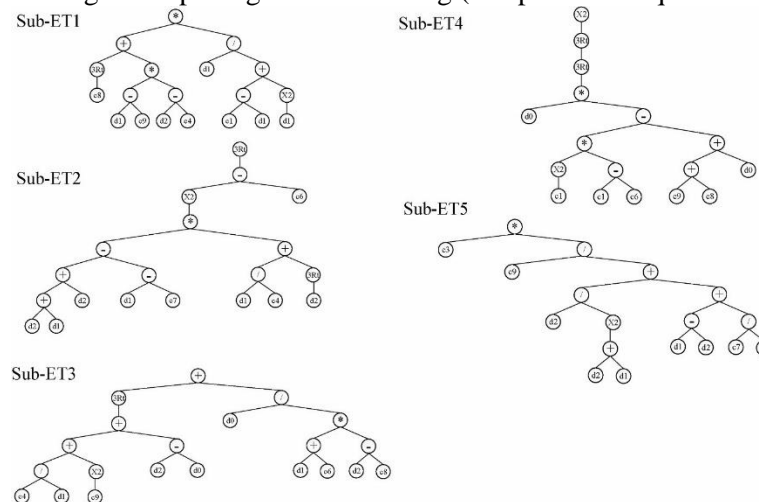


Fig. 6. Expression trees obtained from GEP4 model used in the development of mathematical equation.

Rationalization of the input parameters

Like any other form of concrete, the mechanical qualities of foamed concrete are optimised by the composition of the mixture and the material attributes. The compressive strength of foamed concrete is its most significant quality in terms of mechanical performance. Numerous studies have shown that when foamed concrete's density rises, so does its compressive strength. The density of FC's microstructure

lowers because of its high void volume, which results in a decreased compressive strength. Based on the literature that is currently accessible, the impacts of the characteristics and ratios of the power material on the characteristics of the FC have been extensively examined. According to several studies [89,90], the density of the produced FC and its compressive strength are directly correlated. This connection is made possible by the fact that FC is favoured as a construction material due to its low density. FCs with densities ranging from 400 to 1600 kg/m³ have a strength of 1–10 MPa and can be used to backfill bridge abutments, fill voids, stabilise structures, and provide insulation. has further underground uses, like insulating buildings and slabs [91]. The water/cement (w/c) ratio, another crucial mixture design factor that affects the compressive strength of FCs, has been observed to have an ideal range for mortar and paste between 0.5 and 0.6. However, the water requirement falls with the addition of a superplasticizer, resulting in an ideal w/c between 0.17 and 0.19 [91]. Other research [92,93] have noted that the w/c ratio has an important influence on the compressive strength of FC because it provides impressive paste fluidity, which results in an equal distribution of foam and increases strength. The sand/cement (s/c) ratio has an inversely proportional link to FC's compressive strength. The density of foamed concrete is determined by the amount of foam used, but the compressive strength is determined by the amount of sand. In order to achieve optimum efficacy and provide enough mix strength without losing the desired reasons for both economically and practically installing such concrete, FC's sand content must be thoroughly optimised [94].

Using new algorithms

This study used artificial neural networks (ANNs), gene expression programming (GEP), and gradient boost trees (GBT) to assess the foamed concrete's compressive strength capability. A high-level summary of the machine-learning modelling techniques employed in this work is provided in this section.

Gradient boosted trees (GBT)

Gradient-boosted tree (GBT) models are a collection of regression or classification tree models. These ensemble forward-learning systems deliver anticipated outcomes by progressively raising estimations. A reliable nonlinear regression method for improving tree accuracy is boosting. An ensemble of weak prediction models is created by gradually applying weak classification algorithms to gradually changing data, leading to the production of a series of decision trees. While adding more trees increases accuracy, it also slows the process down and makes it more challenging for humans to grasp. The gradient boosting method generalises the tree boosting methodology to overcome these issues. A strong classifier is created by GBT by combining a number of weak base classifiers. GBT accomplishes global convergence of the algorithm by following the direction of classification, in contrast to conventional techniques that take both positive and negative sample weights into consideration. Using the dataset x_i, y_i, n $i=1$ and an N-dimensional vector of real values as input, call the SoftMax function to generate an N-dimensional vector with real values (0, 1) that add up to 1. A gradient descent technique is used to follow the path of the negative gradient in order to guarantee convergence of the GBT model. $H(x)$, where $x_i = (x_{1i}, x_{2i}, \dots, x_{qi})$, q is the number of predicted parameters, and y_i is the predicted parameter, is a representation of the weak base learner. The GBT model follows a step-by-step process for training the datasets that is

Gene expression programming (GEP)

Many researchers have used gene expression programming (GEP), a flexible and soft computing method that combines genetic programming and gene algorithms. diverse uses in engineering. Numerous engineering applications have used GEP to create empirical equations for evaluating various qualities of concrete made from various materials. When developing a model, the genetic programming (GP) technique disregards prior iterations of preexisting associations [95,96]. A more recent addition, GEP is an extension of GP that uses samples or tiny programmes to encode fixed-length linear chromosomes. To address the shortcomings of the GP approach, Ferreira introduced the GEP technique [97]. The main changes were that only the genome was passed on to the next generation and that single chromosomes could generate entities made up of genes with head and tail portions [98]. Expression trees (ET) are the

name given to these things. The genetic replication of DNA molecules serves as the inspiration for GEPs [99]. The number of accessible chromosomes, which in turn regulates the population size, affects the computing time of GEP. Chromosome diversity is aided by genetic operators. The best-performing chromosome is passed on to following generations, and the cycle repeats itself until a suitable level of fitness is reached [100].

Artificial neural network (ANN)

Artificial neural networks (ANNs) are algorithms that resemble the connections between the neurons that make up a biological nervous system's internal framework (neurons) [101–104]. ANN is a computational and mathematical approach used, like other ML algorithms, to mimic the relationships between the input parameters and output variable(s) [102]. The feedforward neural network is the most prevalent form of neural network, and the most The multilayer perceptron (MLP), which has an input layer, one or more hidden layers, and output layer (s), is a frequently used kind. There is no link between the neurons present in each layer, despite the fact that the quantity of neurons deployed in each layer relies on several factors. Depending on the input and output variables, different models require different numbers of input and output neurons. The hidden layer is where computing occurs. This layer contains a variety of neurons, the number of which must be calculated in order to produce the desired response [105]. The neural network is trained by introducing data to the input and output layers and building the necessary models. By evaluating the discrepancy between the output projected values and actual values, the network's weights and biases were changed to attain the lowest possible error [106]. In the majority of cases, an ANN is an adaptive system that may alter its model in response to pertinent data that is transmitted across the network during the learning phase.

3. Results and discussions

3.1. Predictive performance and validation

3.1.1. ANN

A visual comparison of the experimental and anticipated compressive strength values using the suggested ANN-based model is depicted in Fig. 7. The effectiveness of the developed AI model is improved by the points' proximity to the regression line (1:1 plot) [116]. The effect of the input parameters on forecasting the compressive strength is precisely captured by the ANN model. The training and validation datasets' correlation values are 0.988 and 0.960, respectively, indicating a significant connection between experimental and anticipated outcomes [117]. However, it was also shown that R is insensitive to multiplying and dividing the compressive strength [118], therefore the RMSE and MAE indices were assessed to more accurately assess the model's performance. The much lower values of these performance indices (RMSE_{training} = 2.18, RMSE_{validation} = 2.80, MAE_{training} = 1.71, MAE_{validation} = 2.07) further support it. The compressive strength errors vary from zero to 1.4 MPa, according to the error analysis plot in Fig. 8. The tracing of actual and ANN-modeled compression strength values in Fig. 9a, which represents data points from 0 to 8 and 25 to 32, reveals greater discrepancies primarily in two places.

3.1.2. GEP

The language of genes and expression trees (ETs) are connected, and understanding one aids in understanding the other, claims Ferreira [111]. Typical ETs for the GEP algorithm of the defined models are shown in Fig. 6 to help identify the straightforward empirical correlations for computing compressive strength. Six key mathematical functions may be seen in the sub-ETs (1-3) of concrete's compressive strength: +, x, y, z, 3Rt, and x2. The mechanism of these sub-ETs is based on the head size (hs), which can be calculated using equations (15) and (16), controlling their maximum width and depth (w_{max} and d_{max}, respectively).

such that amin represents the minimum arity, or the smallest possible arguments for the functions, and amax represents the maximum arity, or the greatest possible arguments, respectively. In this study, all developed AI models were given an amin value of zero and an amax value of two.

The GEP model was created, and the ETs were then decoded to produce a straightforward mathematical equation for compressive strength as a function of the chosen input parameters. The Karva notation or Kexpression [119] was converted into ETs and then decoded in line with the hyperparameter values for the GEP model to produce Eq. (17), below, a simple mathematical equation:

$$fc = A + B + C + D + E \text{ Eq. 17}$$

Concrete's compressive strength may be readily calculated using these formulae [120, 121]. In Fig. 7, the suggested GEP-formulated model's experimental vs anticipated compressive strength values are represented graphically. It is important to note that, in contrast to the other two AI approaches used here, the validation dataset's results were superior to those of the training datasets. At larger R values, there is a significant connection between the input variables [118,122]. Regarding the GEP model's correctness, it was noted that the differences in all performance indices taken into consideration (R, RMSE, and MAE) in the training and validation datasets were negligibly small, at 0.004, 0.17, and 0.055, respectively. This demonstrates that the error scatter's concentration is close to zero. Additionally, the error analysis graph in Fig. 8 shows that the compressive strength exhibits errors between 0.3 and 0.3 MPa, demonstrating the created GEP model's superior performance. The tracing of the experimental and GEP-modeled output values in Fig. 9 demonstrates a reduced variation between the results, however a little divergence was seen for datapoints 0-5, 10-15, and 24-30.

3.1.3. GBT

In Fig. 7c, the experimental and projected compressive strength values utilising the proposed GBT prediction model are represented graphically. All three performance indicators beat the ANN and GEP models. It is clear that the R values for the training and validation datasets, 0.980 and 0.977, respectively, are practically similar. Comparing the MAE numbers (2.184 and 1.817) to the RMSE values (2.8555 and 2.690 for the training and validation sets, respectively), the difference was greater. Similar to this, Fig. 8c's error analysis plot demonstrates that the compressive strength has uncertainties between unity and 1.7 MPa. The tracing of experimental and GBT modelled values can finally be seen in Fig. 9c, where the variations in both values are dispersed, in contrast to the ANN and GEP approaches, and can thus be recorded for six small ranges of the data points, including 7-13, 15-17, 23-25, 28-32, 36-38, and 41-44.

3.2. Comparison of the models

A radar plot comparison of the generated models is shown in Fig. 10. Compared to other charts, a radar plot is better at communicating information, especially when there is more data [123]. A spoke projecting from the study's focal point served as a representation of each model under investigation. The radar plot often has a circular layout. The three AI models under investigation were arranged in a triangle. The scale of each series is represented by smaller triangles. In the case of R, the distance between the two triangles was 0.05, but for MAE and RMSE, it was 0.5. To collect multivariate data, some researchers have employed radar plots in a variety of domains [124,125]. The GBT model fared better in the validation phase, with R = 0.977, when assessing the correlation between the observed and predicted values. With an R-value of 0.98, the GBT model likewise demonstrated good agreement throughout training. The ANN and GEP models produced comparable correlation findings; however, the ANN model was somewhat overfitted during training, resulting in a lower correlation than the training model. The GEP model did not exhibit overfitting (Fig. 10a and c). Figs. 10b and 9d provide a comparison of the models' errors. For the validation data, the GBT model had the lowest MAE and RMSE at 1.817 MPa and 2.69 MPa, respectively. The GEP model came in third when examining accuracy, whereas the ANN model trailed the GBT model in terms of accuracy. The predicted-experimental ratios were included to the comparison of the derived models (Table 7). In this comparison, 100% of the validation records for ANN models are

within 20%, compared to 78.26 and 80.4%, respectively, for the GEP and GBT models, for data points with 20%.

The GBT model has been utilised for parametric analysis even though the ANN model performs better in this area than it does the GBT model, which is owing to other positive statistical indices performance.

The performance of the GBT model was also contrasted with that of earlier research projects. Based on 220 experimental findings from the literature, Dao et al.'s [77] traditional ANN evaluation of the compressive strength of FC. Although a comparable performance was attained, w/c ratio and s/c ratio optimisation were not looked into. Ly et al.'s [18] investigation of an ANN model using 375 data points resulted in a maximum R value of 0.959. However, the optimised combined impact of the input factors was not given. The influence of each input parameter was evaluated in the form of partial dependency plots, determining the growing or lowering trend of compressive strength with change input variable. The analysis presented here details each variable's precise contribution at various densities, w/c ratios, and s/c ratios.

3.3. Sensitivity and parametric analysis

Due to the GBT model's robustness, parametric and sensitivity analysis were carried out on the simulated dataset (Table 8). As illustrated in Table 8, simulated data were created by changing one input parameter between its extremes while keeping the remaining variables at their average levels. The stepwise variation in the relative contribution of the input factors and the change in compressive strength with an increase in foam concrete density are shown in Figs. 11 to 13. The compressive strength rose approximately linearly with rise in density at fixed w/c ratio of 0.416 and s/c ratio of 1.04, as illustrated in Fig. 14. The relative contribution of density increased with increasing density, as seen in Fig. 11 The compressive strength was adversely affected by the s/c ratio of 1.04, which was considerably worse in low-density concrete than in high-density concrete. A w/c ratio of 0.41 made a negligible initial contribution to raising density, but when concrete's density was high, it had a detrimental impact on compressive strength. The compressive strength first rose with an increase in the w/c ratio up to 0.35. As can be seen in Fig. 14, a further increase in the w/c ratio significantly reduced the compressive strength. Additionally, Fig. 12 illustrates how raising the w/c has a detrimental effect. Beyond 0.6, w/c increased without contributing to compressive strength. According to Figs. 13 and 14, a rise in s/c had a detrimental effect on the foamed concrete's compressive strength as well.

4. CONCLUDING REMARKS

The results of three prediction models—ANN, GEP, and GBT—that can calculate the compressive strength of foamed concrete (FC) are presented in this study. Since the amount of input factors utilised in the equations limits the experimental data that can be used to calibrate empirical models for estimating the compressive strength of FC, these models' predictions are often extrapolative. Once more, prediction using an empirical model necessitates empirical constants that are challenging to find when characterising the intricate connection between mixture proportions and compressive strength. With respect to the three AI models, this study concentrated on input variable optimisation using a more reliable prediction model. From this investigation, the following results were reached. The density of the FC and compressive strength were strongly positively correlated, according to Pearson's correlation coefficients. The compressive strength of FC exhibited a somewhat negative association with the sand to cement ratio, but a high negative correlation with the water-cement ratio. A very accurate AI model-based parametric and sensitivity analysis was also used to validate the Pearson's correlation results. The Levenberg-Marquardt technique with one hidden layer and 10 neurons was used to optimise the constructed model and produce the best ANN model outcomes. By altering the number of chromosomes, the head size, and the number of genes, the data learned using the GEP algorithm were evaluated in a number of experiments. The optimum hyperparameters for GEP were 200, 12, and 5, respectively, for chromosomes, head size, and the number of genes. The best GBT model was produced using 90 trees, seven maximum depths, and a learning rate of 0.10. When evaluating the performance of the AI models, all of the models produced

correlations of R that were considerably higher than 0.8, ranging from 0.971 to 0.988 for the training data and 0.96 to 0.977 for the validation data, demonstrating a good agreement between the experimental and projected outcomes. The GBT model yielded the highest correlation (0.977) in the validation data as well as the lowest MAE and RMSE (2.184 and 2.85, respectively) for the validation data. So, in terms of accuracy, the GBT model was superior to the other models, followed by the ANN and GEP models, respectively. However, because the GBT model expresses the target variable as a straightforward mathematical connection, its importance cannot be ignored. Maximum concrete strength was attained at a w/c ratio range of 0.35 to 0.40 at an average value of density and s/c ratio during the change in the amount of water in parametric analysis. The compressive strength is significantly reduced when the s/c value is higher than 0.4. The density of the concrete, followed by the w/c and s/c ratios, played a significant influence in influencing the compressive strength of the FC, according to parametric and sensitivity studies. In order to forecast the compressive strength of FC using 232 experimental records gathered from the literature, the present models used three inputs. According to the authors, fresh prediction models should be created based on a variety of experimental data gathered from a single source.

References

- [1] M. Shariati, D.J. Armaghani, M. Khandelwal, J. Zhou, M. Khorami, Assessment of longstanding effects of fly ash and silica fume on the compressive strength of concrete using extreme learning machine and artificial neural network, *J. Adv. Eng. Computation* 5 (2021) 50–74 <https://doi.org/10.25073/JAEC.202151.308>.
- [2] M. Shariati, M.S.Mafipour, B. Ghahremani, F. Azarhomayun, M. Ahmadi, N. T. Trung, A. Shariati, A novel hybrid extreme learning machine–grey wolf optimizer (ELM-GWO) model to predict compressive strength of concrete with partial replacements for cement, *Eng. Comput.* 38 (2022) 757–779, <https://doi.org/10.1007/S00366-020-01081-0/TABLES/7>.
- [3] M. Amran, Y.H. Lee, N. Vatin, R. Fediuk, S. Poi-Ngian, Y.Y. Lee, G. Murali, Design efficiency, characteristics, and utilization of reinforced foamed concrete: a review, *Crystals* 10 (2020) 948, <https://doi.org/10.3390/CRYST10100948>, 10 (2020) 948.
- [4] Y.H.M. Amran, N. Farzadnia, A.A.A. Ali, Properties and applications of foamed concrete; a review, *Construct. Build. Mater.* 101 (2015) 990–1005, <https://doi.org/10.1016/J.CONBUILDMAT.2015.10.112>.
- [5] D. Falliano, D. de Domenico, G. Ricciardi, E. Gugliandolo, Experimental investigation on the compressive strength of foamed concrete: effect of curing conditions, cement type, foaming agent and dry density, *Construct. Build. Mater.* 165 (2018) 735–749, <https://doi.org/10.1016/J.CONBUILDMAT.2017.12.241>.
- [6] D. Niu, L. Zhang, Q. Fu, B. Wen, D. Luo, Critical conditions and life prediction of reinforcement corrosion in coral aggregate concrete, *Construct. Build. Mater.* 238 (2020), 117685, <https://doi.org/10.1016/J.CONBUILDMAT.2019.117685>.
- [7] X. Tan, W. Chen, J. Wang, D. Yang, X. Qi, Y. Ma, X. Wang, S. Ma, C. Li, Influence of high temperature on the residual physical and mechanical properties of foamed concrete, *Construct. Build. Mater.* 135 (2017) 203–211, <https://doi.org/10.1016/J.CONBUILDMAT.2016.12.223>.
- [8] S. Kilincarslan, M. Davraz, M. Akça, The effect of pumice as aggregate on the mechanical and thermal properties of foam concrete, *Arabian J. Geosci.* 11 (2018) 1–6, <https://doi.org/10.1007/S12517-018-3627-Y>, 11. 11 (2018).
- [9] R.K. Dhir, M.D. Newlands, Aikaterini McCarthy, INTRODUCTION TO FOAMED CONCRETE: WHAT, WHY, HOW?, 2005, p. 158, <https://doi.org/10.1680/UOFCIC.34068.0001>.
- [10] A. Hajimohammadi, T. Ngo, P. Mendis, T. Nguyen, A. Kashani, J.S.J. van

- Deventer, Pore characteristics in one-part mix geopolymers foamed by H₂O₂: the impact of mix design, *Mater. Des.* 130 (2017) 381–391, <https://doi.org/10.1016/J.MATDES.2017.05.084>.
- [11] A.A. Sayadi, J.v. Tapia, T.R. Neitzert, G.C. Clifton, Effects of expanded polystyrene (EPS) particles on fire resistance, thermal conductivity and compressive strength of foamed concrete, *Construct. Build. Mater.* 112 (2016) 716–724, <https://doi.org/10.1016/J.CONBUILDMAT.2016.02.218>.
- [12] S. Sidhardhan, A. Sagaya Albert, [Experimental investigation on light weight cellular concrete by using glass and plastic waste—a review](https://doi.org/10.1016/J.IJST.2020.09.014), *Int. J. Sci. Technol. Res.* 9 (2020) 1947–1952.
- [13] A.M. Hameed, R.F. Hamada, Using the glass and rubber waste as sustainable materials to prepare foamed concrete with improved properties, in: *IOP Conference Series: Materials Science and Engineering*, 2020, <https://doi.org/10.1088/1757-899X/881/1/012188>.
- [14] H.Y. Tiong, S.K. Lim, Y.L. Lee, C.F. Ong, M.K. Yew, Environmental impact and quality assessment of using eggshell powder incorporated in lightweight foamed concrete, *Construct. Build. Mater.* 244 (2020), <https://doi.org/10.1016/j.conbuildmat.2020.118341>.
- [15] L.S. Kang, F.K. Poh, L.F. Wei, T.H. Yong, L.Y. Ling, L.J. Hock, K.Y. Jin, Acoustic properties of lightweight foamed concrete with eggshell waste as partial cement replacement material, *Sains Malays.* 50 (2021) 537–547, <https://doi.org/10.17576/jsm-2021-5002-24>.
- [16] A.A. Jhatial, W.I. Goh, N. Mohamad, K.H. Mo, A. Mehroz, Thermomechanical evaluation of sustainable foamed concrete incorporating palm oil fuel ash and eggshell powder, *J. Eng. Res. (Kuwait)* 9 (2021) 64–79, <https://doi.org/10.36909/jer.v9i3A.8290>.
- [17] M.F. Omar, M.A.H. Abdullah, N.A. Rashid, A.L.A. Rani, Partially replacement of cement by sawdust and fly ash in lightweight foam concrete, *IOP Conf. Ser. Mater. Sci. Eng.* 743 (2020), 012035, <https://doi.org/10.1088/1757-899X/743/1/012035>.
- [18] H.-B. Ly, M.H. Nguyen, B.T. Pham, Metaheuristic optimization of Levenberg–Marquardt-based artificial neural network using particle swarm optimization for prediction of foamed concrete compressive strength, *Neural Comput. Appl.* 33 (2021) 17331–17351, <https://doi.org/10.1007/S00521-021-06321-Y>, 24. 33 (2021).
- [19] D. Falliano, D. de Domenico, G. Ricciardi, E. Gugliandolo, Key factors affecting the compressive strength of foamed concrete, *IOP Conf. Ser. Mater. Sci. Eng.* 431 (2018), 062009, <https://doi.org/10.1088/1757-899X/431/6/062009>.
- [20] A.M. Neville, *Properties of Concrete*, 2011.
- [21] M.R. Jones, [Foamed concrete for structural use](https://doi.org/10.1016/B978-0-08-100811-1.00001), in: *Proceedings of One Day Seminar on Foamed Concrete: Properties, Applications and Latest Technological Development*, 2001, pp. 27–60.
- [22] R. Othman, R.P. Jaya, K. Muthusamy, M. Sulaiman, Y. Duraisamy, M.M.A. B. Abdullah, A. Przybył, W. Sochacki, T. Skrzypczak, P. Vizureanu, A.V. Sandu, Relation between density and compressive strength of foamed concrete, *Materials* 14 (2021) 2967, <https://doi.org/10.3390/MA14112967>.
- [23] C. Bing, W. Zhen, L.N.-J. of materials in civil engineering, undefined 2012, Experimental research on properties of high-strength foamed concrete, *Ascelibrary.Org.* 24 (2012) 113–118, [https://doi.org/10.1061/\(ASCE\)MT.1943-5533.0000353](https://doi.org/10.1061/(ASCE)MT.1943-5533.0000353).
- [24] L. de Rose, J. Morris, *The Influence of Mix Design on the Properties of Microcellular Concrete*, 1999. https://books.google.com/books?hl=en&lr=&id=e7pFNxUOKkC&oi=fnd&pg=PA185&ots=DrkiqCyu7&sig=m0ehQy1WTbex5ydtMm_X9ESmdBo. (Accessed 5 November 2021).
- [25] K.C. Brady, R.A. Watts, I.R. Jones, [Specification for Foamed Concrete](https://doi.org/10.1016/B978-0-08-100811-1.00001), 2001.

- [26] Y.H.M. Amran, N. Farzadnia, A.A.A. Ali, Properties and applications of foamed concrete; a review, *Construct. Build. Mater.* 101 (2015) 990–1005, <https://doi.org/10.1016/J.CONBUILDMAT.2015.10.112>.
- [27] A. Raj, D. Sathyan, K.M. Mini, Physical and functional characteristics of foam concrete: a review, *Construct. Build. Mater.* 221 (2019) 787–799, <https://doi.org/10.1016/J.CONBUILDMAT.2019.06.052>.
- [28] J. Zhang, J. Li, L. Zhang, Z. Liu, Z. Jiang, Dynamic performance of foam concrete with recycled coir fiber, *Frontiers Mater.* 7 (2020) 320, <https://doi.org/10.3389/FMATS.2020.567655/BIBTEX>.
- [29] Y.H. Mugahed Amran, R. Alyousef, H. Alabduljabbar, M.H.R. Khudhair, F. Hejazi, A. Alaskar, F. Alrshoudi, A. Siddika, Performance properties of structural fibred- foamed concrete, *Results Eng.* 5 (2020), <https://doi.org/10.1016/j.rineng.2019.100092>.
- [30] K. Ramamurthy, E. Nambiar, G.R. C, concrete, undefined, *A Classification of Studies on Properties of Foam Concrete*, Elsevier, 2009 (n.d.), <https://www.sciencedirect.com/science/article/pii/S0958946509000638>. (Accessed 5 November 2021).
- [31] A. Just, B.M.-M. characterization, undefined, *Microstructure of High-Strength Foam Concrete*, Elsevier, 2009 (n.d.), <https://www.sciencedirect.com/science/article/pii/S1044580308003392>. (Accessed 5 November 2021).
- [32] N. Uddin, F. Fouad, U.K. Vaidya, A. Khotpal, J.C. Serrano-Perez, Structural characterization of hybrid fiber reinforced polymer (FRP)-Autoclave aerated concrete (AAC) panels, *Http://Dx.Doi.Org/10.1177/0731684406065090*. 25, <https://doi.org/10.1177/0731684406065090>, 2016, 981-999.
- [33] S. Mindess, *Developments in the formulation and reinforcement of concrete* (accessed November 5, 2021), <https://books.google.com/books?hl=en&lr=&id=YGGdDwAAQBAJ&oi=fnd&pg=PP1&dq=S.+Mindess+,+Developments+in+the+Formulation+and+Reinforcement+of+Concrete,+Wood+head+Publishing+and+Maney+Publishing,+Institute+of+Materials,+Minerals++Mining+CRC+press+Boca+Raton+Boston+New+York+Washington,+DC,+Elsevier,+2014.&ots=1dYAFvb9oy&sig=TMT40zAIt0rKAc8fJ9IZFflxFdQ>, 2019.
- [34] P. Tikalsky, J. Pospisil, W.M. C, concrete research, undefined, *A Method for Assessment of the Freeze–Thaw Resistance of Preformed Foam Cellular Concrete*, Elsevier, 2004 (n.d.), <https://www.sciencedirect.com/science/article/pii/S0008884603003909>. (Accessed 5 November 2021).
- [35] M. Jones, A.M. the international conference held at, undefined 2005, *Behaviour and assessment of foamed concrete for construction applications*, *Icevirtuallibrary.Com* (n.d.), <https://www.icevirtuallibrary.com/doi/abs/10.1680/uofcic.34068.0008>. (Accessed 5 November 2021).